Desalination, 49 (1984) 1—15
Elsevier Science Publishers B.V., Amsterdam — Printed in The Netherlands

APPLIED SIMILARITY CRITERIA IN THE SCALE-UP FROM EXISTING TO LARGE MSF DESALINATION PLANTS

D. BARBA

Facoltà di Ingegneria, Università de L'Aquila, 67100 L'Aquila (Italy)

AND

S. ARAZZINI AND G. MIGLIORINI

Italimpianti SpA, Piazza Piccapietra 9, 16121 Genova (Italy)

(Received August 9, 1983)

SUMMARY

The trend of building large desalination water stations with a large number of parallel units of 5—6 migd each is critically examined. The opportunity to increase unit size to 12—13 migd for cross tube and to 20—25 migd for long tube geometry has been discussed previously [1]. In this paper optimal sizes analyzed for cross tube and for long tube geometry are 12 migd and 18 migd respectively, and the similarity criteria, that can be used for design purposes starting from the behavior of two reference industrial plants (5 migd cross tube and 8 migd long tube respectively), are illustrated.

The scale-up from existing units is based on the similarity of evaporator parameters: brine specific flow rate, flashdown, Froude number at entrance of the stages, dimensionless vapor velocity at the brine release surface, dimensionless vapor velocity through the demisters, two phases flow parameters at the cross-section below the distillate channel (only for cross tube geometry), dimensionless stage length defined as the ratio between actual and critical length.

The designs of new large units, characterized by process and geometrical features similar to the reference plants based on these profiles, allows the same water purity and performance ratio for the new capacities.

An economic analysis on a standard 6 migd unit shows that the investment cost/m^3/d is is about 20% lower for 12 migd cross tube and 30% lower for 18 migd long tube plants.

0011-9164/84/$03.00

SYMBOLS

BFR	— brine specific flow rate, T/h m
C_p	— brine specific heat, kcal/h m^2 °C
Fr	— Froude number, dimensionless
h	— distillate channel height above evaporator floor, m
H_{ND}, H_{RP}	— discharge orifice height for New Design and Reference Plant respectively, m
k_T	— turbulent thermal conductivity of brine, kcal/h m°C
K	— constant defined by Eq. (5)
L_{ND}, L_{RP}	— brine channel width for New Design and Reference Plant respectively, m
P, p'	— stage pressure, kg/m^2 and dimensionless respectively
Pr	— Prandtl number, dimensionless
R	— gas constant, kcal/kg °K
Re	— Reynold's number, dimensionless
T, T'	— point temperature of brine, °C and dimensionless respectively
T_{eq}	— stage equilibrium temperature of brine, °C
T_i	— stage inlet temperature of brine, °C
u, u'	— horizontal component of the point turbulent velocity of brine, m/s and dimensionless respectively
U	— brine average velocity in the stage, m/s
U_i	— brine velocity at discharge orifice, m/s
U_{ND}, U_{RP}	— brine velocity at discharge orifice for New Design and Reference Plant respectively, m/s
v, v'	— vertical component of the point turbulent velocity of brine, m/s and dimensionless respectively
V_B	— brine velocity inside tubes, m/s
V_S	— vapor velocity in the stage, m/s
V	— vapor flow rate in the stage, kg/h
W_{ND}, W_{RP}	— brine flow rate for New Design and Reference Plant respectively, kg/h
x, x'	— stage horizontal coordinate, m and dimensionless respectively
X_{cr}	— stage critical length, m
X_B, Y_B	— Baker parameters defined by Eq. (11)
y, y'	— stage vertical coordinate, m and dimensionless respectively
Y	— stage brine depth, m
z_F	— vapor velocity defined by Eq. (10), dimensionless
z_{FD}, z_{FB}	— vapor velocity at demister and brine release surface respectively, dimensionless

Greek symbols

α	— constant of Baker's parameter defined by Eq. (12)
Δ	— temperature drop or flashdown between stages, °C

Δ_{ND}, Δ_{RP} — temperature drop or flashdown between stages for New Design and Reference Plant respectively, °C
λ — water latent heat of vaporization, kcal/kg
μ — discharge orifice coefficient
μ_L — brine viscosity, centipoise
ν_T — turbulent kinematic viscosity of brine, m^2/h
ρ_V, ρ_L — vapor and brine density respectively, kg/m^2
σ — superficial tension of brine, dine/cm
ψ — constant of Baker's parameter defined by Eq. (12)

INTRODUCTION

The present trend to realize large desalted water stations with a large number of parallel units (generally 5 migd capacity each) does not appear to be based either on economic or technological considerations. As a matter of fact on the one hand the cost of the desalination station decreases when the capacity of the single unit is increased. On the other hand, the state-of-the-art allows for the design of reliable higher capacity units.

In a previous work [1] on the optimum range of capacity for large units, analysis has shown that the cross tube geometry allows a maximum capacity of about 12 migd due to technological limitations, there are no theoretical or technological restrictions for the capacity of long tube geometry plants.

TABLE I

SCALE-UP OF NEW DESIGN PLANTS COMPARED TO REFERENCE PLANTS

	Cross tube	Long tube
Large New Design units proposed		
migd	12	18*
tbt	110	110
PR	8	8
Reference Plants		
	Ras Abu Fontas (Qatar) Started 1979	Porto Torres (Sardinia, Italy) Started 1973
migd	5	8
tbt	112	115
PR	7.5	7.5

*Capacity a little lower than 20 migd to better satisfy the similarity criterion.

The limitations derive from economic considerations that define an optimum size to be in the range 20—25 migd.

A similarity criterion is now illustrated that allows the scaling-up of units of this capacity starting with known industrial units [2, 3, 4] (Table I).

UNIFIED SIMILARITY CRITERION

The scale-up from the existing Reference Plants to the large size units is based on a similarity criterion, making it possible to obtain new designs with the minimum deviation in the similarity parameters whose values are derived from the running plants. These parameters are analyzed through the three main figures of a MSF plant: 1) distillate output, 2) distillate purity and 3) performance ratio.

1. Distillate output

Once the top and bottom brine temperatures are fixed, the distillate output is a function of the recirculating brine flow rate. The parameters that characterize the correct evaporator sizing referred to the recirculating brine flow rate are

— Brine flow rates per width of brine channel (BFR). Typical profiles derived from the Reference Plants are given in Fig. 1 as a function of the brine temperature.

— Brine velocity inside tubes (V_B). In the cross tube geometry V_B will be selected so that the bundle length is equal to the brine channel width. In

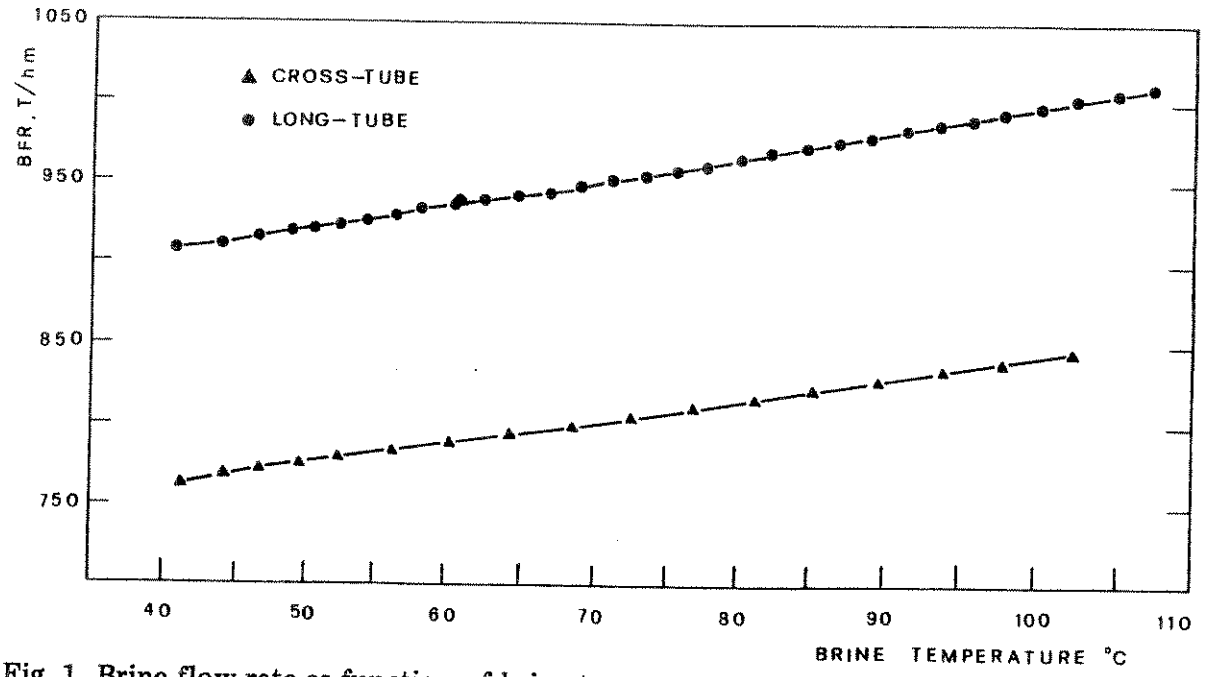

Fig. 1. Brine flow rate as function of brine temperature along the evaporators.

long tube geometry, this velocity is assumed so as to make equal the lengths of the tube bundle and of the stage:

Cross tube Reference Plant $V_B = 1.8 \div 2.1$ m/s
Long tube Reference Plant $V_B = 1.8 \div 2.1$ m/s

2. Distillate purity

While a theoretical prediction of the product purity is a remarkably complex and partly unsolved problem, the same prediction becomes easy when, at design stage, it is possible to refer to an existing unit in commercial operation. In the latter case the design problem is that of keeping in similarity the following points: type of flash, vapor velocity at release surface, vapor velocity through the demisters, type of two-phase flow under the distillate channel (only for cross tube geometry).

The following parameters are examined.

Type of flash

The phenomena inside a flash chamber, taking into account both the fluidodynamic and the mass transfer aspects, can be described by a simplified system of partial differential equations including the continuity equation, the horizontal component of the momentum balance equation, and the energy balance equation respectively [5].

$$\frac{\partial u}{\partial x} + \frac{\partial v}{\partial y} = 0$$

$$u\frac{\partial u}{\partial x} + v\frac{\partial u}{\partial y} = -\frac{1}{\rho_L}\frac{\partial P}{\partial x} + \nu_T \frac{\partial^2 u}{\partial y^2} \qquad (1)$$

$$u\frac{\partial T}{\partial x} + v\frac{\partial T}{\partial y} = \frac{k_T}{\rho_L C_p}\frac{\partial^2 T}{\partial y^2}$$

where the unknown functions u, v, are respectively the horizontal and vertical components of the point turbulent velocity and T is the point temperature of the brine.

The integration of the above system satisfying the related boundary and initial conditions for an absolute forecasting of u, v and T is a remarkably complex problem, asking for significant simplifying hypotheses that often cause the solution to be unreliable. On the contrary, it is by far easier to make use of the system (1) in order to identify the conditions of similarity.

The geometrical coordinates, the point velocity components, the pressure and the brine point temperature, can be made dimensionless by using respec-

tively the following reference parameters: brine average depth inside the chamber, Y, brine average velocity, U, stage equilibrium temperatures, T_{eq}, and Reynolds number, Re.

Introducing in Eqs. (1) the dimensionless parameters:

$$x' = \frac{x}{y} \qquad y' = \frac{y}{Y}\,\mathrm{Re}^{1/2}$$

$$u' = \frac{u}{U} \qquad v' = \frac{v}{U}\,\mathrm{Re}^{1/2} \tag{2}$$

$$p' = \frac{P}{\rho_L U^2} \qquad T' = \frac{T}{T_{eq}}$$

the system [1] can be made dimensionless and the unknown functions, solving the partial differential system, can be expressed as:

$$\frac{u}{U} = \varphi_1\left[\frac{x}{Y}, \frac{y\,\mathrm{Re}^{1/2}}{Y}, \frac{P(T_{eq})}{U^2}, \mathrm{Pr}\right]$$

$$\frac{v\,\mathrm{Re}^{1/2}}{U} = \varphi_2\left[\frac{x}{Y}, \frac{y\,\mathrm{Re}^{1/2}}{Y}, \frac{P(T_{eq})}{U^2}, \mathrm{Pr}\right] \tag{3}$$

$$\frac{T}{T_{eq}} = \varphi_3\left[\frac{x}{Y}, \frac{y\,\mathrm{Re}^{1/2}}{Y}, \frac{P(T_{eq})}{\rho_L U^{2\prime}}, \mathrm{Pr}\right]$$

where Pr is the Prandtl number.

Whatever their form, Eqs. (3) and the boundary conditions, nondimensionalized, represent a general "family of solutions" exclusively function of the initial conditions, but independent on the particular geometry or system or operating conditions.

Introducing numerical values for the parameters Y, U, T_{eq}, Re, Pr, Eqs. (3) became a particular "family of solutions" representative of a particular evaporator and only function of the initial conditions. As a consequence, in order to compare two evaporators referring to the type of flash and to the stage efficiency, and in order to compare the behavior of u, v and T inside corresponding stages, it is mandatory to examine:

— numerical values of the similarity parameters Y, U, T_{eq}, Re and Pr along the evaporators,

— boundary and initial conditions, that is the temperature and the velocity at the stage inlets.

a) Similarity parameters. The physical system under consideration is the same in both evaporators (flashing brine at about 65000 ppm TDS) and the

comparison is made between stages at about the same brine temperature; it follows that the equality of T_{eq}, of the physical characteristics and of the Pr number is nearly verified.

For the other parameters, the following considerations can be drawn:

— the design average brine depth Y will be assumed equal for the two designs,

— the average brine velocities U and the Re numbers along the evaporators will be similar due to the similarity of BFR profiles and of the Y value.

As a consequence we can conclude that in the range of experimental errors, the same set of numerical values of Y, U, T_{eq}, Re, Pr is representative of both the Reference Plant and the New Design.

b) Boundary and initial conditions. The boundary conditions are identical in both systems, as they are characteristic of the considered phenomenon and do not depend on the single evaporator when the equality for Y is assumed. Study of the initial conditions can be reduced to that of the interstage flashdown. As a matter of fact, the inlet temperature T_i can be expressed as

$$T_i = T_{eq} + \Delta \tag{4}$$

and the inlet velocities depend on the velocities at the discharge orifices U_i, which can be expressed as:

$$U_i^2 = \mu^2 \frac{2 g_c \lambda P}{\rho_L R (T_{eq} + 273)^2} \Delta = K \Delta \tag{5}$$

We can conclude that for each couple of corresponding stages a couple of particular solutions exists in the "family solutions" (Eq. (3)), each characterized by its own flashdown value.

Typical flashdown profiles for Reference Plants are given in Fig. 2. In conclusion the similarity for the type of flash is assured when the similarity for BFR, Y and Δ is verified.

The above analysis describes the phenomenon along a stage, but system (3) cannot describe the shape of the free surface at the stage inlet, because it does not include the vertical component of the momentum balance equation.

However, similarity from this point of view is governed by the Froude number at the discharge orifice that can be expressed utilizing Eq. (5) as

$$\mathrm{Fr} = \frac{U_i^2}{gH} = \frac{K}{g} \frac{\Delta}{H} \tag{6}$$

where H is the orifice height. Making Fr equal for the two projects, it follows

$$\frac{H_{ND}}{H_{RP}} = \frac{\Delta_{ND}}{\Delta_{RP}} \tag{7}$$

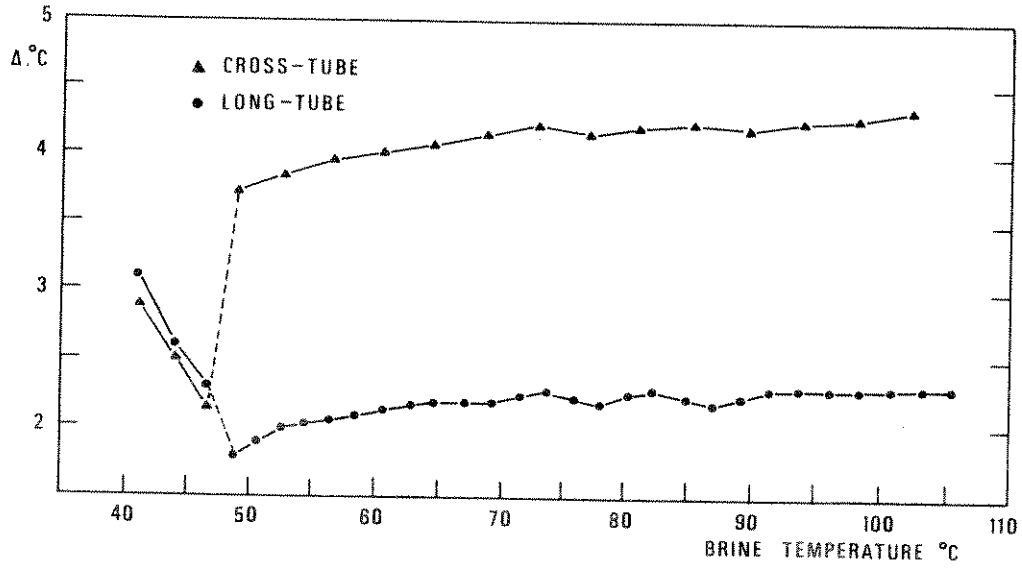

Fig. 2. Flash-down as function of brine temperature along the evaporators.

where *ND* represents the conditions of New Design and *RP* those of the Reference Plants.

At the same time the velocities ratio can be expressed as

$$\frac{U_{ND}}{U_{RP}} = \frac{(L\,H/W)_{RP}}{(L\,H/W)_{ND}} = \left[\frac{\Delta_{ND}}{\Delta_{RP}}\right]^{0.5} \tag{8}$$

where W is the brine flow rate and L is the total width available for the orifices. Introducing Eq. (7) into Eq. (8) we have

$$\frac{L_{ND}}{L_{RP}} = \left[\frac{\Delta_{RP}}{\Delta_{ND}}\right]^{1.5} \frac{W_{ND}}{W_{RP}} \tag{9}$$

that represents the similarity condition for Fr number to be verified for New Design.

Vapor velocity at the release surface and vapor velocity through the demisters

The dimensionless velocity characterizing the entrainment phenomenon as a function of pressure/temperature of the stages is

$$Z_F = 14.4\,\frac{V_S}{(\rho_L - \rho_V/\rho_V)^{1/2}} \tag{10}$$

This parameter has been assumed in order to examine the similarity at the vapor release and through the demisters.

In Fig. 3 the dimensionless velocities z_{FB} (at the release surfaces) and z_{FD} (at the demisters) have been represented as functions of the brine temperature for the Reference Plants.

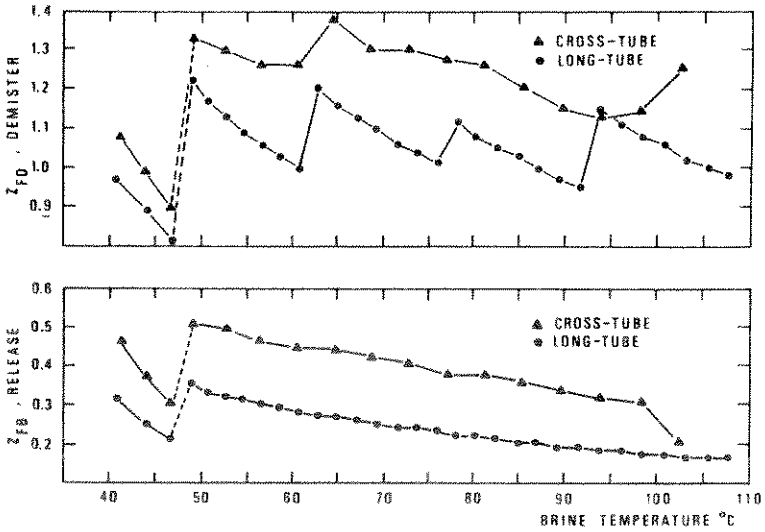

Fig. 3. Dimensionless vapor velocity through the demisters and at release surface as function of brine temperature.

Geometrical parameters. In order to complete the analysis of the similarity with reference to product purity the two geometrical parameters which must be considered are the height of the demisters from stage floor, and the distillate channel bottom height from the stage floor.

The first parameter together with z_{FB} characterizes the quantity of entrained liquid at the demisters inlet and will be made equal for the two plants.

The distillate channel height does not affect the phenomenon in the long tube geometry, whereas the vapor distribution between the two demisters symmetrical zones is governed by this parameter in the cross tube geometry. In this case the similarity of the kind of two phase flow under the distillate channel must be verified.

Baker's parameters, made similar along the evaporators, make it possible to have the same representative points in the regions of horizontal two phase flow. Baker's parameters X_B and Y_B are given by [6]

$$X_B = \frac{W\alpha\psi}{V} \qquad Y_B = \frac{V}{4.87\ \mathrm{Lh}\alpha} \tag{11}$$

where

$$\alpha = \left[\frac{\rho_V}{1.2}\ \frac{\rho_L}{1000}\right]^{0.5} \qquad \psi = \frac{73}{\sigma}\left[\mu_L\left(\frac{1000}{\rho_L}\right)^2\right]^{0.33} \tag{12}$$

The profile representative of the kind of two phase flow along the cross tube Reference Plant is given on Fig. 4, showing the Baker's graph. Fig. 4 evidentiates that the profile is contained in the region of stratified two phase flow, condition for a good vapor distribution between the two demister symmetrical zones.

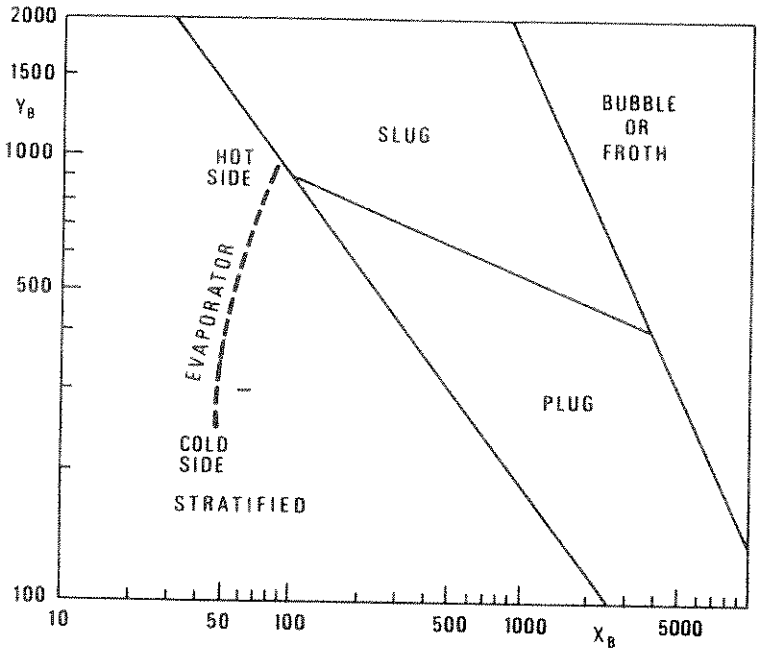

Fig. 4. Type of two-phase flow under the distillate channel along the cross tube evaporator.

3. Performance ratio

As far as the PR is concerned, the similarity is verified as a consequence of the use of the same correlations for the computation of clean heat transfer coefficients. Moreover the designs will be in similarity, since the temperature losses are approximately equal as a consequence of the similarity between the parameters discussed above. As a matter of fact, the temperature losses that reduce the logarithmic mean temperature difference can be classifed as:

— boiling point elevation BPE
— temperature losses across the demister and the tube bundle
— non-equilibrium allowance, i.e. stage efficiency.

The BPE values along the evaporators are nearly the same if the comparison is made as previously state, between stages working with brines at the same concentrations and at nearly equal temperatures. The similarity in Z_{FD}

profile implies nearly equal vapor losses, the pressure drop across the tube bundle being negligible.

As far as the stage efficiency is concerned, the similarity is verified. In fact, the similarity implies the same field of brine temperatures in corresponding stages, so that we can expect the same non-equilibrium allowance. Moreover taking into account that the significant variation of the brine temperature occurs for values of the stage longitudinal coordinate x lower than stage critical length X_{cr}, a further criterion to verify this point is to keep in similarity the stage lengths made dimensionless by their own X_{cr}. Fig. 5 shows the dimensionless stage lengths obtained by the use of the formula derived in [7] for the computation of X_{cr}.

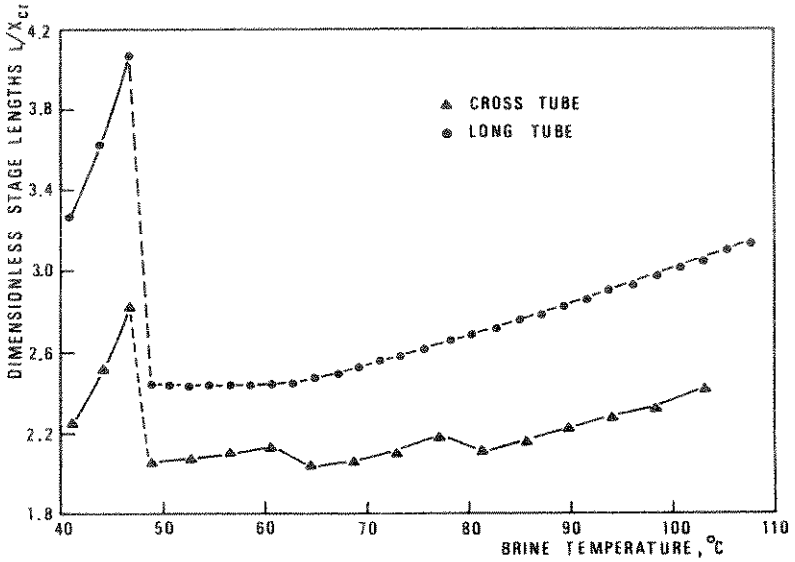

Fig. 5. Dimensionless stage lengths as function of brine temperature.

CHARACTERISTICS OF LARGE UNITS ACCORDING TO THE SIMILARITY PARAMETERS

The use of the above parameters allows us to scale-up the basic figures characterizing the geometry of the two following large size units:

— Cross tube geometry 12 migd capacity, 110° tbt, 8.0 performance ratio.

— Long tube geometry 18 migd capacity, 110° tbt, 8.0 performance ratio.

Common design conditions for the two projects are the following:

Sea water temperature	30°C
Sea water TDS	45,000 ppm
Antiscale treatment	improved chemicals

Fouling factors	
Heat recovery	0.000175 kcal/h m^2 °C
Heat reject	0.000206 kcal/h m^2 °C
Distillate purity	< 55 μs/cm

Using the above design conditions, various geometries have been tested for each type of evaporator to select the best design for reducing the deviations from the similarity parameters.

In other words this aim has been reached by an optimization program that guides the main program to minimize an objective function represented by a combination of the differences between the calculated similarity parameters and the values of the corresponding figures from Reference Plants.

A comparison of the main geometric characteristics for the two units is given in Table II. A schematic general assembly of the evaporators and their outer dimensions are shown in Fig. 6 where the cross tube evaporator is conceived on two tiers and the long tube evaporator on three tiers due to its lower typical stage height.

TABLE II

CROSS TUBE AND LONG TUBE DESIGN CHARACTERISTICS

	Cross flow	Long flow
Capacity (migd)	12	18
Performance ratio	8.0	8.0
No. of stages		
Recovery section	18	28
Reject section	3	3
Heat exchange surface (m^2)		
Recovery section	108,850	134,260
Reject section	19,100	20,680
Tube bundle characteristics		
Tubes no. (recovery/reject)	2,339/2,464	11,214/8,638
Tube diameter (mm)	38.1	25.4
Tube thickness	1.22	1.22
Bundle dimensions (m)		
Width	2.0	2.0
Height	2.3	2.3
Length	21.6	30
Module geometry		
Width	21.5	28
Height	3.9	3.0
Length	49	30
No. of bundles per modules	1	2
No. of modules	2	6

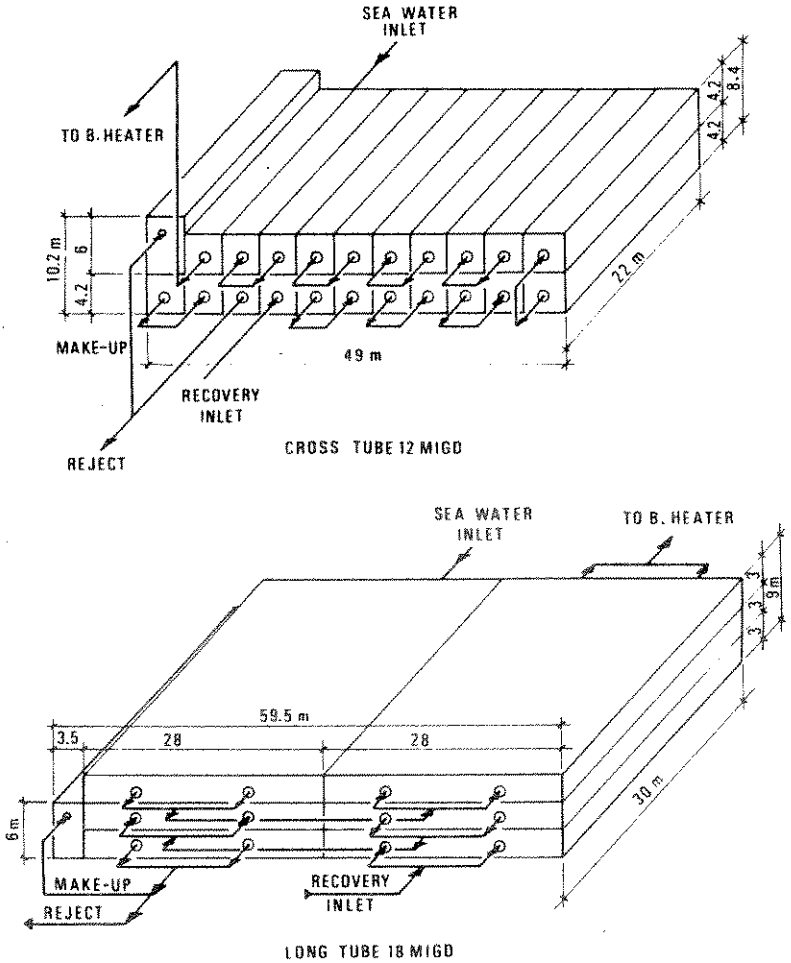

Fig. 6. Schematic general assembly of cross and long tube evaporators.

ECONOMIC COMPARISON

The investment costs for both above solutions have been evaluated on turnkey basis. As far as the scope of works is concerned the following items have been taken into account in the economical computation:

— Evaporator and auxiliaries (brine recirculation, blowdown and distillate systems)
— Sea water supply system including chlorine treatment
— Steam supply and condensate treatment
— Electrical system
— Instrument and control system
— Spare parts

The choice of evaporator materials was made based on the following assumptions:

Tubes	CuNi 66/30 2Fe 2Mn
	Al Brass
Plates	CuNi 90/10
	Naval Brass
Shell	C.S. CuNi 90/10 cladded
	C.S.
Demisters	AISI 316 L
Water boxes	C.S. CuNi 90/10 cladded
Internals	AISI 316 L
Non-condensable extraction system	AISI 316 L

The comparison of investment costs with reference to a typical unit of 6 migd is given in Fig. 7 where three solutions are also compared to produce 36 migd of fresh water.

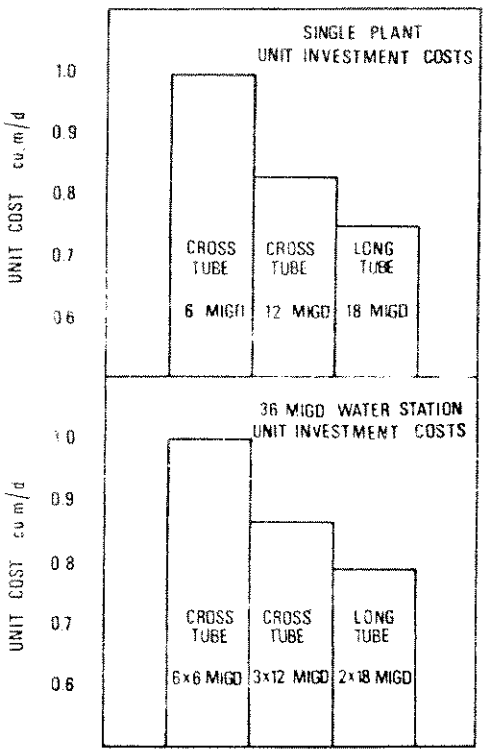

Fig. 7. Unit investment cost for single unit and for 36 migd water station.

CONCLUSIONS

The similarity criterion here shown allows the design of large MSF units cross and long tube type satisfying the reliability aspects. According to a previous general analysis of large size plants, two configurations have been illustrated:

— A crosstube 12 migd unit that satisfies the similarity criteria with reference to a 5 migd industrial plant installed in Qatar.

— A long tube 18 migd unit in similarity with a 8 migd Porto Torres Plant in Italy.

A preliminary cost analysis on a 6 migd plant shows that the investment cost per m^3/d is about 20% lower for 12 migd cross tube and 30% lower for 18 migd long tube. As a consequence, a water station of 36 migd using large units allows a saving per m^3/d of 15% for a cross tube, and of 26%, for a long tube MSF unit.

REFERENCES

1. D. Barba, D. Bogazzi, A. Germana' and G. Tagliaferri, Analysis of Large Desalination Plants, Desalination, 33 (1980) 1—10.
2. D. Barba, G. Liuzzo, G. Spizzichino and G. Tagliaferri, Porto Torres Desalting Plants, Proc. 5th Int. Symp. on Fresh Water from the Sea, Alghero, 2 (1976) 39—48.
3. D. Barba, G. Liuzzo and G. Tagliaferri, Mathematical Model for Multi-Flash Desalting Plant Control, 4th Int. Symp. on Fresh Water from the Sea, Heidelberg, 1 (1973) 153—168.
4. D. Barba, A. Germana', A. Salemme, G. Tagliaferri and E. Zonetti, Qatar Desalination Plants, Desalination, 26 (1978) 109—116.
5. Development of an Analytical Model of a Flash Stage, Office of Saline Water, R&D Progress Rept. 503, (1969).
6. Saline Water Conversion Engineering Data Book, Office of Saline Water, Dept. of Interior, No. 357 (1968) pp. 1—2.
7. Chamber Geometry in Multi-Stage Flash Evaporator, Office of Saline Water, R&D Progress Rept. No. 108 (1964).